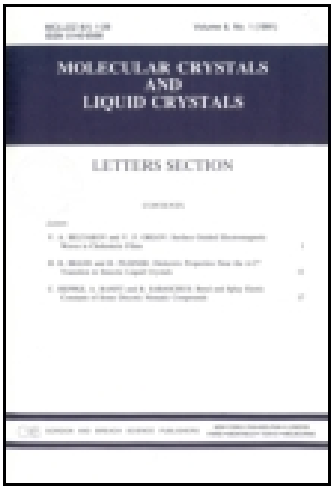

Molecular Crystals and Liquid Crystals
Publication details, including instructions for authors and subscription information:
http://www.tandfonline.com/loi/gmcl20

Influence of Fe_2O_3 Doping on TiO_2 Electrode for Enhancement Photovoltaic Efficiency of Dye-Sensitized Solar Cells

Tae Sung Eom[a], Kyung Hwan Kim[a], Chung Wung Bark[a] & Hyung Wook Choi[a]

[a] Department of Electrical Engineering, Gachon University, Sujeong-Gu, Seongnam-Si, Gyeonggi-Do, Korea

Published online: 17 Nov 2014.

To cite this article: Tae Sung Eom, Kyung Hwan Kim, Chung Wung Bark & Hyung Wook Choi (2014) Influence of Fe_2O_3 Doping on TiO_2 Electrode for Enhancement Photovoltaic Efficiency of Dye-Sensitized Solar Cells, Molecular Crystals and Liquid Crystals, 600:1, 39-46, DOI: 10.1080/15421406.2014.936769

To link to this article: http://dx.doi.org/10.1080/15421406.2014.936769

Mol. Cryst. Liq. Cryst., Vol. 600: pp. 39–46, 2014

ISSN: 1542-1406 print/1563-5287 online
DOI: 10.1080/15421406.2014.936769

Taylor & Francis
Taylor & Francis Group

Influence of Fe_2O_3 Doping on TiO_2 Electrode for Enhancement Photovoltaic Efficiency of Dye-Sensitized Solar Cells

TAE SUNG EOM, KYUNG HWAN KIM,
CHUNG WUNG BARK, AND HYUNG WOOK CHOI*

Department of Electrical Engineering, Gachon University, Sujeong-Gu, Seongnam-Si, Gyeonggi-Do, Korea

In this work, we report for the first time the improvement of the photovoltaic characteristics of dye-sensitized solar cells (DSSCs) by doping TiO_2 with Fe_2O_3. DSSCs were fabricated using various percentages of Fe_2O_3-doped TiO_2 composite nanoparticles. The Fe_2O_3-doped DSSCs exhibited a maximum conversion efficiency of 5.76% because of the effective electron transport. DSSCs based on Fe_2O_3-doped TiO_2 films showed better photovoltaic performance than cells fabricated with only TiO_2 nanoparticles. This result was attributed to the prevention of recombination between electrons in the TiO_2 conduction band with the dye or electrolytes. A mechanism was suggested based on impedance results, which indicated improved electron transport at the interface of the TiO_2/dye/electrolyte.

Keywords DSSCs; Fe_2O_3-doping; TiO_2; photovoltaic performance; electron recombination

Introduction

Dye-sensitized solar cells (DSSCs) based on nanocrystalline TiO_2 semiconductors are of great interest as alternatives to conventional solar cells because of their low production cost and high performance [1–4]. DSSCs are composed of a dye-adsorbed nanoporous TiO_2 layer on a fluorine-doped tin oxide (FTO) glass substrate, redox electrolytes, and a counter electrode. The system is chiefly composed of a mesoporous TiO_2 film comprising nanometer-sized particles with a large specific surface area. However, an unusual feature of this type of DSSCs is the lack of a space charge layer, which separates the injected electrons from the holes in the dye or electrolyte [5–8]. A unidirectional charge flow with no electron leakage at the interfaces is essential for high energy-conversion efficiency [9].

In addition, the synthesis of TiO_2 nanomaterials for DSSCs and the studies of their photoelectric properties have attracted much attention. In recent years, some researchers have found that doping and mixing the TiO_2 film with metal ions could be a promising

*Address correspondence to Prof. Hyung Wook Choi, Department of Electrical Engineering, Gachon University, 1342 SeongnamDaero, Sujeong-Gu, SeongNam, Gyeonggi-do, 461-701 Korea (ROK). Tel.: (+82)31-750-5562; Fax: (+82)31-750-8833. Email: chw@ gachon.ac.kr

Color versions of one or more of the figures in the article can be found online at www.tandfonline.com/gmcl.

approach to improve the electron transfer in the TiO_2-based nanostructured electrodes of DSSCs [10]. It has been reported that the efficiency of DSSCs can be improved by surface modification of TiO_2 with insulating oxides or high-band-gap semiconductors to form a blocking layer, thus preventing charge recombination at the TiO_2/dye/electrolyte interface [11–14].

In this paper, we first report the improvement of the photovoltaic characteristics of DSSCs by the doping of TiO_2 with Fe_2O_3. Fe_2O_3 doping reduced the surface trap states of TiO_2, suppressed charge recombination, and increased the driving force of electron injection, thereby improving the power conversion efficiency. The impedance results indicated an improved electron transport at the TiO_2/dye/electrolyte interface. DSSCs were fabricated by application of Fe_2O_3-doped and TiO_2 composite nanoparticles in various proportions. As a result, the DSSCs based on Fe_2O_3-doping showed better photovoltaic performance than cells made purely of TiO_2 nanoparticles.

Experimental

Titanium(IV) isopropoxide (TTIP, Aldrich Chemical), ethyl alcohol, nitric acid, and deionized (DI) water were used as the starting materials. TiO_2 powders were manufactured by a sol-gel method, and TiO_2 pastes were prepared as per the literature [15–16]. Nanoporous TiO_2 upper layers were coated on the passivating-layer-coated FTO glass by the doctor blade method. The prepared TiO_2 electrode was sintered at 450°C for 15 min and then at 500°C for 15 min in air.

Fe_2O_3-doped TiO_2 films were prepared from ferric oxide (Fe_2O_3 nanopowder, 50 nm, Aldrich), with stoichiometric ratios ranging from 0.5 to 10 wt% in TiO_2.

The nanoporous TiO_2 electrode films were immersed in an N719 dye complex for 24 h at room temperature. A counter electrode was prepared by spin-coating a H_2PtCl_6 solution onto the FTO glass and heating it at 450°C for 30 min. The dye-adsorbed TiO_2 electrode and the Pt counter electrode were assembled onto a sandwich-type cell and sealed with a 60-μm-thick hot-melt sealant. An electrolyte solution was introduced through a drilled hole in the counter electrode, which was then sealed with a cover glass.

The morphology and thickness of the prepared passivating layers were investigated using field emission scanning electron microscopy (FE-SEM, S-4700, Hitachi). The conversion efficiency and electrochemical impedance of the fabricated DSSCs were measured using an *I–V* solar simulator (Solar Simulator, McScience). The active area of the resulting cell exposed to light was approximately 0.25 cm^2 (0.5 cm × 0.5 cm). The absorbance of the TiO_2 thin films was measured using a UV spectrometer (UV-Vis 8453, Agilent).

Results and Discussion

Figure 1(a) shows the XRD pattern of the Fe_2O_3 and Figure 1(b) shows the XRD pattern of the TiO_2 powder at 500°C, revealing a mixture of anatase and rutile phases. In the Fe_2O_3 phase, the XRD pattern [Fig. 1(c)] shows that the Fe_2O_3-doped TiO_2 surface was sufficient to crystallize the forms (F1–F3). The XRD pattern of Fe_2O_3 showed prominent Fe_2O_3 peaks, denoted as F1 (220), F2 (311), and F3 (400), which were compared with JCPDS (25-1402).

The FE-SEM analysis revealed the TiO_2 nanoparticles prepared by the sol-gel method have consistent diameters of 20–30 nm (Figure 2(a)), and the diameters of the Fe_2O_3 nanoparticles prepared by the same method were consistently within the range 40–60 nm (Figure 2(c)). A mixture of the TiO_2 and Fe_2O_3 surfaces could be observed in Figure 2(b).

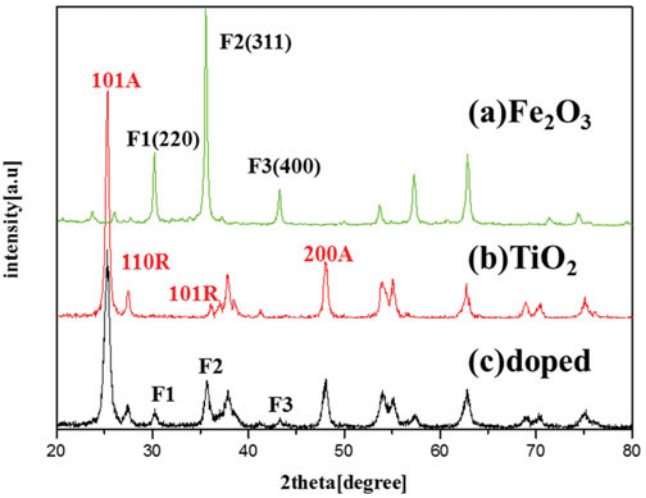

Figure 1. XRD patterns of Fe_2O_3-doped films: (a) Fe_2O_3, (b) TiO_2, and (c) Fe_2O_3-doped TiO_2.

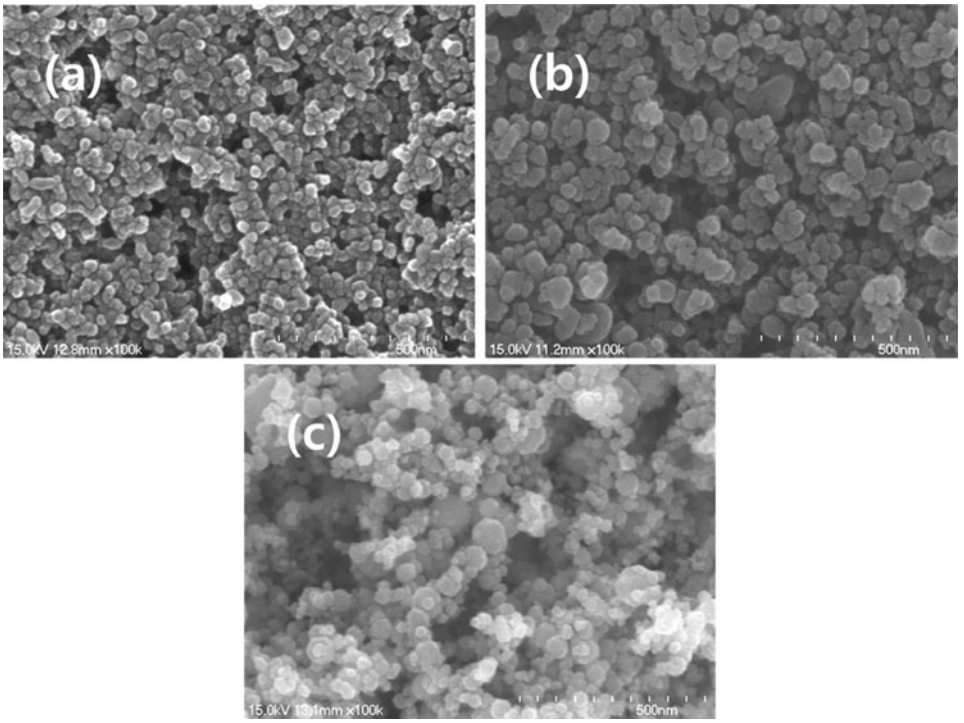

Figure 2. FE-SEM images of Fe_2O_3-doped TiO_2 films: (a) TiO_2 (b) Fe_2O_3-doped TiO_2, and (c) Fe_2O_3.

The SEM results showed that the grain size of the Fe_2O_3 nanoparticles was larger than that of the TiO_2 nanoparticles.

The Fe_2O_3-doped samples are presented in Nyquist plots in Figure 3. Electrochemical impedance spectroscopy (EIS) is used to investigate electron transport and recombination in DSSCs. In general, the impedance spectrum of a DSSC shows three semicircles in the frequency range 10 mHz–100 kHz. The first semicircle (R1) is related to change transfer at the counter electrode, which is measured in the kHz range. The second semicircle (R2) is related to electron transport in the TiO_2/dye/electrolyte interface around 1–100 Hz. The third semicircle shows the Warburg diffusion process of I^-/I_3^- in the electrolyte [17–19]. The small semicircle is fitted to the charge-transfer resistance (R1) and a constant phase, and the large semicircle is fitted to the transfer resistance (R2) and a constant phase. Because R1 is not affected by Fe_2O_3, we can mainly focus on R2. The first semicircle was a minimum for the Fe_2O_3 (1 wt%), which was related to the charge-transfer resistances of the FTO/TiO_2 and the TiO_2/electrolyte interfaces (R2). The decreased R2 of Fe_2O_3 (1 wt%) indicated a reduction in electron recombination and increased electron transport efficiency. However, in the case of increased Fe_2O_3 (10 wt%), R2 was increased, because the Fe_2O_3 (10 wt%) with more trap sites obstructed the movement of electrons from the nanoporous TiO_2 layer to the FTO electrode. It seems that the electron flow improved because the Fe_2O_3 co-semiconductor reduced the resistance (even at the counter electrode) due to the efficient applied potential transport.

Fe_2O_3 doping impacted the UV-vis absorbance of the dye-adsorbed TiO_2 films. Figure 4 shows the absorption spectra of the N-719 dye over the 400–800 nm wavelength range for various TiO_2 composite electrode films (0.5–10 wt% Fe_2O_3). Between 400 and 500 nm wavelength, the absorbance of the sample containing 1.0 wt% Fe_2O_3 was the highest, and the absorbance of the sample containing 10 wt% Fe_2O_3 was the lowest. According to the Lambert-Beer's law, a higher absorbance indicates a higher dye concentration. A suitable amount of Fe_2O_3 in the film could provide a large surface area for dye adsorption. Therefore, the TiO_2 layer with the dye serves as a photoactive layer. It is well known that the photocurrent of a DSSC is correlated directly with the number of dye molecules; the

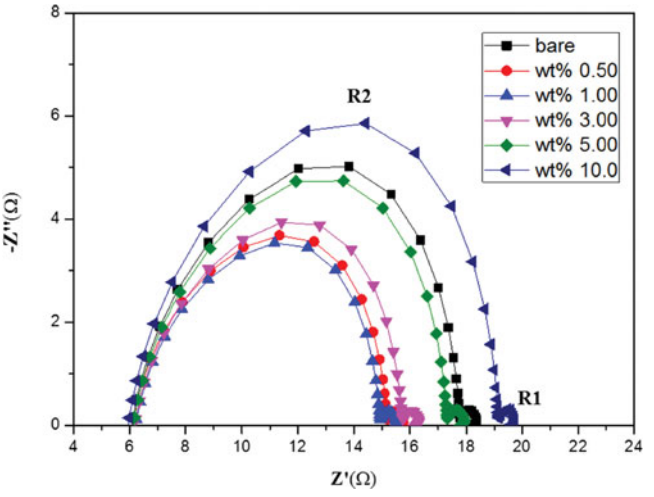

Figure 3. Electrochemical impedance spectra of Fe_2O_3-doped TiO_2 films.

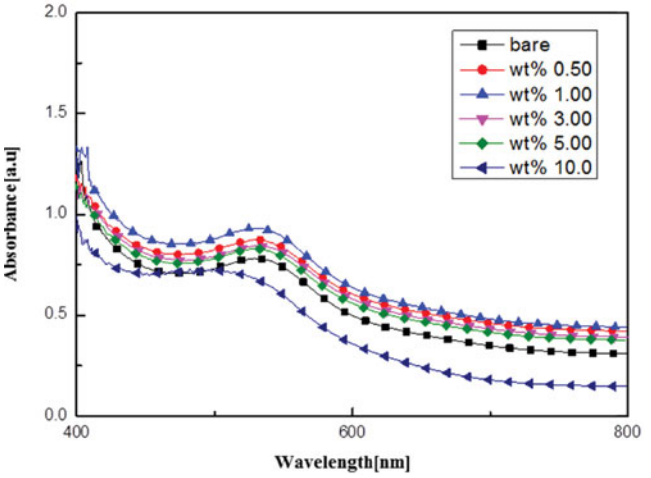

Figure 4. UV-vis absorption spectra of Fe_2O_3-doped TiO_2 films.

increased adsorption of dye molecules leads to an enhanced harvest of the incident light, as well as a larger photocurrent.

Figure 5 shows the *I-V* characteristics of the TiO_2 layers doped with various Fe_2O_3 concentrations. The corresponding photovoltaic parameters of the DSSCs are summarized in Table 1. A DSSC with a light-to-electric energy conversion efficiency of 5.76%, short-circuit current density of 12.6 mA/cm^2, open-circuit voltage of 0.66 V, and fill factor (FF) of 68.78% was achieved. For the 1.0 wt% Fe_2O_3 film, the conversion efficiency was the highest. The internal resistance decreased as a function of Fe_2O_3 doping, which confirmed the previous discussion about the blocking effect of charge recombination by Fe_2O_3 modification, as shown in Fig. 3 (R2). The mechanism for preventing this voltage drop is explained in Fig. 6. The electrons that would flow to the dye or the electrolyte can

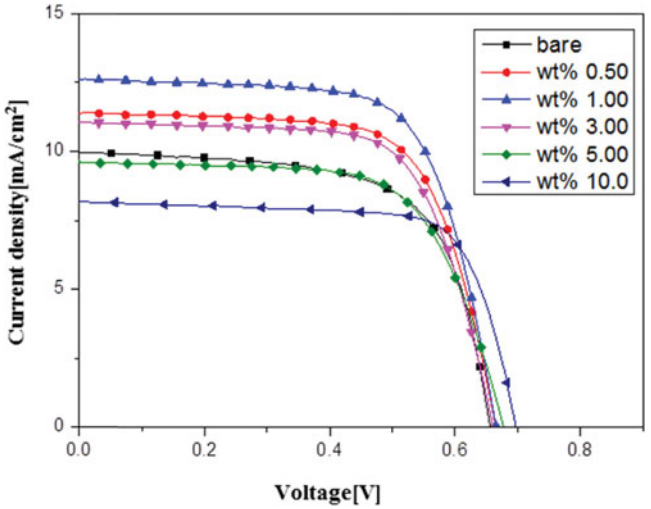

Figure 5. *I-V* characteristics of Fe_2O_3-doped TiO_2 films.

Table 1. J_{sc}, V_{oc}, fill factor (FF), and efficiency (η)

	V_{oc} (V)	J (mA/cm^2)	FF (%)	η (%)
Bare	0.65	9.97	65.90	4.30
0.50 wt%	0.66	11.39	68.41	5.17
1.00 wt%	0.66	12.62	68.78	5.76
3.00 wt%	0.66	11.05	68.53	4.99
5.00 wt%	0.67	9.62	66.07	4.30
10.0 wt%	0.69	8.17	73.24	4.18

be confined to the conduction band (CB) of Fe_2O_3, through which they travel. The open-circuit voltage of DSSCs increased as a function of Fe_2O_3 doping. One of the most important parameters for a solar cell is its photoelectric conversion efficiency. The short-circuit current (J_{sc}) increased significantly because of the effects of the Fe_2O_3 cosemiconductor. It was also beneficial to have a higher FF and useful voltage in the DSSC [20–21]. The FF increased

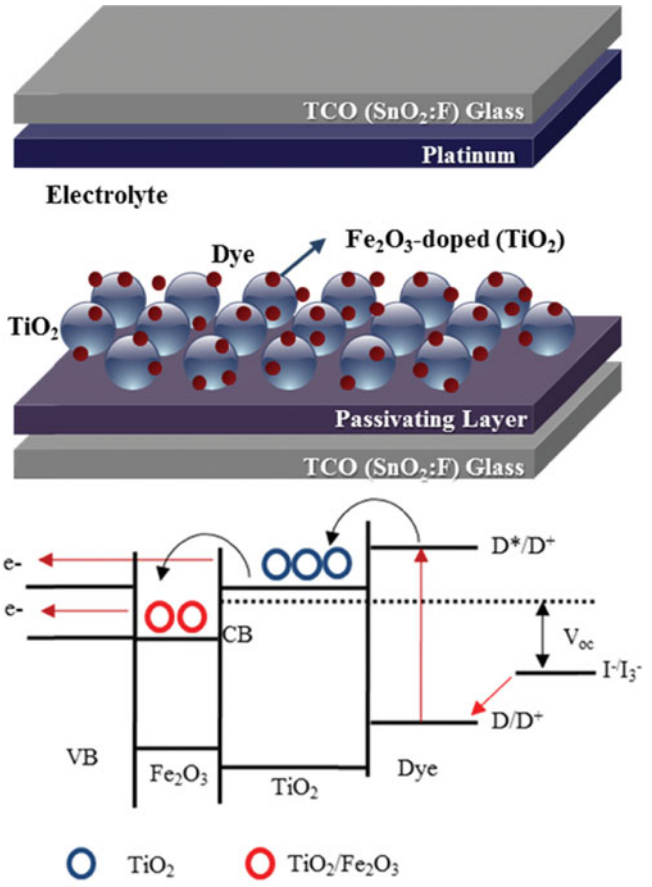

Figure 6. (a) Schematic diagram of flexible DSSC of Fe_2O_3-doped TiO_2 films and (b) suggested mechanism to improve the efficiency of DSSCs prepared by using the Fe_2O_3-doped cells.

from 65% to 68% because of the low-band-gap Fe_2O_3. The Fe_2O_3-doping dependence of the overall conversion efficiency (η) exhibited the same trend as the short-circuit photocurrent. However, higher concentrations of Fe_2O_3 (5.0–10 wt%) reduced the solar cell performance.

Conclusion

In this work, we report for the first time the improvement in the photovoltaic characteristics of DSSCs by doping TiO_2 with Fe_2O_3. DSSCs were fabricated using various percentages of Fe_2O_3 doped into TiO_2 nanoparticles to form composite nanoparticles. The DSSC prepared without Fe_2O_3 had a J_{sc} of 9.97 A/cm^2, V_{oc} of 0.65 V, and η of 4.3%. The DSSC doped with 1.0 wt% Fe_2O_3 had the maximum conversion efficiency (5.76%) because of the effective electron transport. The slightly lower CB of Fe_2O_3 prevented electron trapping effects in the CB of TiO_2. The phenomenon was beneficial in prohibiting the recombination of electrons in the CB of TiO_2 with those in the dye or the electrolyte. It was observed that as the efficiency increased, the internal resistance decreased. Thus, the use of Fe_2O_3-doped TiO_2 films was demonstrated to be an effective method to improve the efficiency of TiO_2-nanoparticle-based DSSCs.

Funding

This work was supported by the Human Resources Development program (No. 20124030200010) of the Korea Institute of Energy Technology Evaluation and Planning(KETEP) grant funded by the Korea government Ministry of Trade, Industry and Energy.This work was supported by the National Research Foundation of Korea (NRF) Grant Funded by the Korean Government (MEST) (No. 2012R1A1A2044472)

References

[1] O'Regan, B., & Grätzel, M. (1991). *Nature*, *353*, 737–740.
[2] Gratzel, M. (2006). *Prog. Photovoltaics: Res. Appl.*, *14*, 429.
[3] Nogueria, A. F., Longo, C., & De paoli, M.-A. (2004). *Coord. Chem. Rev.*, *248*, 1455–1468.
[4] Gregg, B. A. (2004). *Coord. Chem. Rev.*, *248*, 1215–1224.
[5] Chappel, S., Chen, S. G., & Zaban, A. (2002). *Langmuir*, *18*, 3336.
[6] Cahen, D., Hodes, G., Gratzel, M., Guillemoles, J. F., & Riess, I. (2000). *J. Phys. Chem. B*, *104* 2053.
[7] Ni, M., Leung, M. K. H., Leung, D. Y. C., & Sumathy, K. (2006). *Sol. Energy Mater. Sol. Cells*, *90*, 1331.
[8] Chou, C. S., Yang, R. Y., Yeh, C. K., & Lin, Y. J. (2009). *Powder Technol.*, *194*, 95.
[9] Xia, J., Masaki, N., Jiang, K., Wada, Y., & Yanagida, S. (2006). *Chem. Lett*, *35.*
[10] Ko, K. H., Lee, Y. C., & Jung, Y. J. (2005). *J. Colloid Interface Sci.*, *283*, 482.
[11] Alarcon, H., Boschloo, G., Mendoza, P., Solis, J. L., & Hagfeldt, A. (2005). *J. Phys. Chem. B*, *109*, 18483.
[12] Chen, S. G., Chappel, S., Diamant, Y., & Zaban, A. (2001). *Chem. Mater.*, *13*, 4629.
[13] Wang, Z.-S., Huang, C.-H., Huang, Y.-Y., Hou, Y.-J., Xie, P.-H., Zhang, B.-W., & Cheng, H.-M. (2001). *Chem. Mater.*, *13*, 678.
[14] Jung, H. S., Lee, J. K., Nastasi, M., Lee, S. W., Kim, J. Y., Park, J. S., Hong, K. S., & Shin, H. (2005). *Langmuir*, *21*, 10332.
[15] Jin, Y. S., Kim, K. H., Park, S. J., Kim, J. H., & Choi, H. W. (2010). *J. Korean Phys. Soc.*, *57*, 1049–1053.
[16] Jin, Y. S., Kim, K. H., Park, S. J., Yoon, H. H., & Choi, H. W. (2011). *J. Nanosci Nanotechnology.*, *11*, 10971–10975.

[17] Pan, K., Dong, Y., Tian, C., Zhou, W., Tian, G., Zhao, B., & Fu, H. (2009). *Electrochim. Acta*, *54*, 7350–7356.
[18] Bay, L., West, K., Winther-Jensen, B., & Jacobsen, T. (2006). *Sol. Energy Mater. Sol. Cells*, *90*, 341–351.
[19] Mikroyannidis, J. A., Stylianakis, M. M., Roy, M. S., Suresh, P., & Sharma, G. D. (2006). *Sol. Energy Mater. Sol. Cells*, *90*, 341–351.
[20] Qin, Q., Tao, J., & Yang, Y. (2010). *Synth. Met.*, *160*, 1167.
[21] Becker, K. D., Schrader, M., Kwon, H. S., & Yoo, H. I. (2009). *Phys. Chem. Chem. Phys.*, *11*, 3082.